Biophysical Chemistry 165–166 (2012) 62–73

Contents lists available at SciVerse ScienceDirect

Biophysical Chemistry

journal homepage: http://www.elsevier.com/locate/biophyschem

The conformational behavior and H-bond structure of asparagine: A theoretical and experimental matrix-isolation FT-IR study

Bram Boeckx *, Guido Maes

Department of Chemistry, University of Leuven, Celestijnenlaan 200 F, B-3001 Leuven, Belgium

HIGHLIGHTS

- ► Ab initio exploration of the conformational landscape of asparagine.
- ► Three intramolecular H-bonds in the most stable form.
- ► A strong H-bond interaction between the side chain and the backbone.
- ► Experimental identification by matrix-isolation FT-IR spectroscopy.
- ► A mean frequency deviation of 7.6 cm^{-1}.

GRAPHICAL ABSTRACT

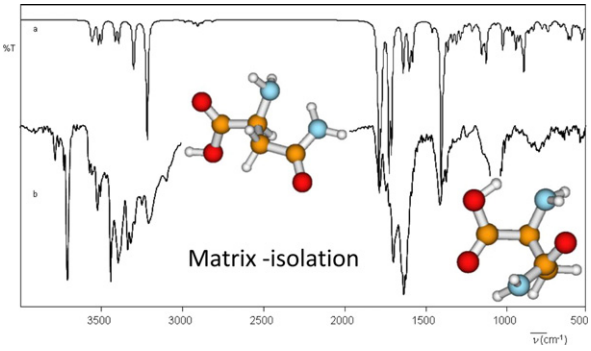

ARTICLE INFO

Article history:
Received 18 February 2012
Received in revised form 11 March 2012
Accepted 12 March 2012
Available online 21 March 2012

Keywords:
Ab initio
Infrared
Cryospectroscopy
Conformations
Amino acid
DFT

ABSTRACT

Due to the high importance of the structural properties of peptides, the conformational behavior of one of their elementary building blocks, asparagine, has been investigated in this work. Matrix-isolation FT-IR spectroscopy is a suitable technique to investigate the intrinsic properties of small molecules. Asparagine has been subjected to matrix-isolation FT-IR spectroscopy supported with DFT and MP2 calculations. DFT optimization of asparagine resulted in 10 stable conformations with $\Delta E_{DFT}<10$ kJ.mol^{-1}. Compared to a previous study, one new conformation has been revealed. Further optimization at the MP2/6-31++G** level resulted in seven conformations with $\Delta E_{MP}<10$ kJ.mol^{-1}. A conformation containing the three intramolecular H-bonds, i.e. $C=O^{sc}\ldots HN^{bb}$, $C=O^{bb}\ldots HN^{sc}$ and $OH^{bb}\ldots N^{bb}$ appeared to be the most stable one at both levels despite the large negative entropy contribution due to these 3 H-bonds. At the sublimation temperature of 353 K, the DFT method predicts four and the MP2 method six conformations to be present in the experimental matrix-isolation spectrum. These conformations have different intramolecular H-bonds, which has allowed to identify at least 4 low energy conformations in the FT-IR spectrum. Detailed comparison between theory and experiment resulted in a mean frequency deviation of 7.6 cm^{-1}.

1. Introduction

One of the most intriguing questions in biophysical chemistry is how protein sequences determine the unique structure. This question, known as the protein folding problem, is of great importance because understanding protein folding mechanisms is a key to successful manipulation of protein structure and most important their functionality, which is directly related to their conformational flexibility [12]. As elementary building block of proteins, the intrinsic conformational properties and energies of amino acids determine, to a large extend, the functionality of proteins and polypeptides [26]. In addition, the amino acid residues in proteins correspond to the low-energy conformations [30].

* Corresponding author. Tel.: +32 16327465; fax: +32 16327992.
E-mail addresses: boeckx@hotmail.com (B. Boeckx), guido.maes@chem.kuleuven.be (G. Maes).

0301-4622/$ – see front matter © 2012 Elsevier B.V. All rights reserved.
doi:10.1016/j.bpc.2012.03.006

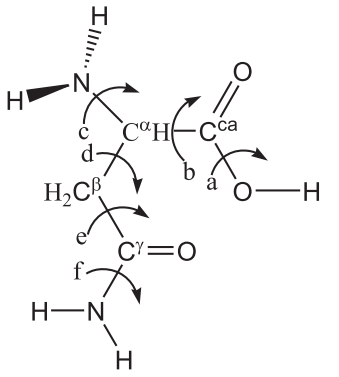

Fig. 1. Numbering and possible internal rotation axes (°) for asparagine.

A very suitable methodology to study the intrinsic properties of small molecules is matrix-isolation FT-IR spectroscopy. In a matrix, a molecule is essentially not involved in any interactions. Furthermore the obtained FT-IR spectra can be possibly used to detect amino acids in interstellar space [35].

Due to the importance of the conformational behavior and energetics of amino acids many of them have been subjected to ab initio studies, e.g. [14,17,19,24,36,37]. All of these studies have revealed more than one stable conformation with four typical kinds of backbone structure characterized by an intramolecular H-bond, i.e. OH…N, NH_2…O=C, NH_2…O(H) and NH_2…O=C. The occurrence of several stable conformations could give rise to very complex FT-IR spectra. This is probably the reason why matrix-isolation FT-IR studies have only been performed for relatively simple amino acids such as glycine [32], alanine [21], isoleucine [6] and cysteine. [11] In this study, the somewhat more complex amino acid asparagine is subjected to a matrix-isolated FT-IR study, supported by a theoretical approach.

The NH_2 group in the side chain of asparagine allows the formation of additional H-bonds. However, it is well known that the amino group in an amide group is an extremely weak base due to considerable resonance so that the side chain proton-acceptor capabilities are only located in the C=O group.

Asparagine was the first amino acid isolated (1806) in its crystalline form from asparagus juice in which it is abundant [39]. Asparagine plays an important role in the metabolic control of cell functions in nerve and brain tissue [25]. It is essential for the synthesis of glycoproteins and a large number of proteins as it is involved in the liver for converting an amino acid into another [1,18,24,29,31].

An extended theoretical ab initio investigation of asparagine has been performed by the group of Lin [10]. A set of 972 conformational trial structures was optimized at successive DFT(B3LYP)/6-311G* and DFT(B3LYP)/6-311++G** levels of theory. 62 stable conformations were found and these were subjected to MP2 single point energy calculations. The shifted vibrations of some H-bond involved stretching modes of the representative conformations have also been reported. The stabilities for side chain conformations of asparagine in solutions have been theoretically studied by Kimura [20]. The asparagine dipeptide has also been theoretically studied using the HF and MP2 methodology by Aleman et al., [1] who have concluded that the gauche conformations are dominant.

As far as experimental data are concerned, IR and Raman spectra of solid asparagine and its ND_3^+ and ND_2 deuterated derivatives have been recorded and a general assignment of the fundamental vibrations has

Table 1
DFT(B3LYP)/6-31++G** and MP2/6-31++G** energies, zero-point vibrational energies (ZPE), relative energies (ΔE) and dipole moments (μ) for the most stable asparagine conformations.

Conformation	Type of backbone	Energy (a.u.)	ZPE[a] (a.u.)	Total energy[b] (a.u.)	ΔE[c] (kJ.mol^{-1})	μ (D)	ΔE[d] (kJ.mol^{-1})
DFT							
ASN1	I $N^{bb}H…O^{sc}+N^{sc}H…O^{bb}$	−492.495198	0.132662	−492.362536	0.00	2.76	0.00
ASN7	I $NH…O^{sc}$	−492.493090	0.131703	−492.361387	3.02	5.04	5.19
ASN2	II $N…HN^{sc}$	−492.493249	0.131932	−492.361317	3.20	3.89	0.51
ASN6	I $NH…O^{sc}$	−492.493029	0.132355	−492.360674	4.89	4.22	5.65
ASN10	IV $OH…O^{sc}$	−492.492234	0.131740	−492.360494	5.36	6.75	8.20
ASNX	I $O..HN^{sc}$	−492.491739	0.132551	−492.359188	8.79	3.31	[e]
ASN3	II $N…HN^{sc}$	−492.491005	0.131868	−492.359137	8.92	4.08	10.63
ASN8	II $NH…O^{sc}$	−492.490041	0.131015	−492.359026	9.22	3.59	12.64
ASN4	II	−492.490027	0.131165	−492.358862	9.65	4.73	12.84
ASN9	III $N…HN^{sc}$	−492.490735	0.131910	−492.358825	9.74	5.44	11.51
ASN5[f]	III	−492.490017	0.131376	−492.358641	10.23	2.24	13.01
MP2							
ASN1	I $N^{bb}H…O^{sc}+N^{sc}H…O^{bb}$	−491.132046	0.135066	−490.996980	0.00	3.28	0.00
ASN2	II $N…HN^{sc}$	−491.128841	0.134205	−490.994636	6.16	4.14	8.58
ASN3	II $N…HN^{sc}$	−491.128719	0.134249	−490.994470	6.59	4.46	10.38
ASN4	II	−491.127798	0.133740	−490.994058	7.67	4.99	12.05
ASN5	III	−491.127581	0.133987	−490.993594	8.89	2.46	12.97
ASN6	I $NH…O^{sc}$	−491.127864	0.134358	−490.993506	9.12	4.20	10.54
ASN7	I $NH…O^{sc}$	−491.127663	0.134341	−490.993322	9.61	5.32	10.96
ASN8	II $NH…O^{sc}$	−491.126501	0.133753	−490.992747	11.11	3.39	15.52
ASN9	III $N…HN^{sc}$	−491.126732	0.134158	−490.992574	11.57	5.75	14.23
ASN10	IV $OH…O^{sc}$	−491.125992	0.133691	−490.992301	12.29	7.02	15.52
ASNX	I $O..HN^{sc}$	−491.125917	0.134893	−490.991024	15.64	3.58	[e]

[a] ZPE values scaled with the uniform scaling factor 0.97.
[b] ZPE corrected energies included.
[c] Energy difference between the different conformations relative to the most stable conformation ASN1.
[d] Values obtained by Chen et al. [10]
[e] No values reported for this conformation. [10]
[f] ASN is included as most stable conformations with amino acid backbone type III.

been proposed [9]. The gas phase structures of cationized asparagine and complexes with Li^+, Na^+, K^+, Rb^+, Cs^+ and Ba^{2+} have been investigated with infrared multiple photon dissociation spectroscopy by the group of Heaton et al. [15,16]. The obtained spectra were compared with the results of DFT calculations. Differences in the NIR spectra of asparagine and glutamine in aqueous media have been found in the range 4570–4350 cm^{-1}. [40]

2. Theoretical methodology

The potential energy surface of asparagine has been explored by the density functional theory (DFT), including Becke's nonlocal hybrid three-parameter exchange functional (B3) [2] in combination with the Lee–Yang–Parr (LYP) [23] correlation functional and in a further stage by the Møller–Plesset second-order perturbation theory [27] (MP2). The optimizations at both levels were performed with the 6-31++G** basisset. The extension of the basisset with diffuse and polarisation functions, has been suggested to be important when studying H-bond sensitive molecules. This method has previously been successfully applied in supporting matrix-isolation FT-IR spectra. As a matter of fact, we have limited the calculations to DFT and MP2 and have not used computational more expensive methods. Frequency calculations of the most stable conformations were performed by the same method. The obtained frequencies and the zero-point energies (ZPE) were corrected for the anharmonicity with earlier optimized variable scaling, i.e. 0.95 for ν(X-H), 0.98 for γ and τ, 0.975 for all other modes and 0.97 for the ZPE [38]. The theoretical DFT intensities and frequencies were used to simulate the theoretical spectra taking into account the relative MP2 abundance of each conformation and using Lorentzian line shapes with 2 cm^{-1} full width at half height. The computational calculations (optimizations, energy calculations and frequency analyses) were performed using the Gaussian 03 software package [13]. The potential energy distributions (PED) of each vibrational mode were calculated using a special software package designed by Dr. L. Lapinski (Institute of Physics, Pol. Acad. of Sciences, Warsaw, Poland) [33]. This theoretical approach has been successfully applied in the past for the analysis of matrix-isolation spectra of similar molecules [4–8,28].

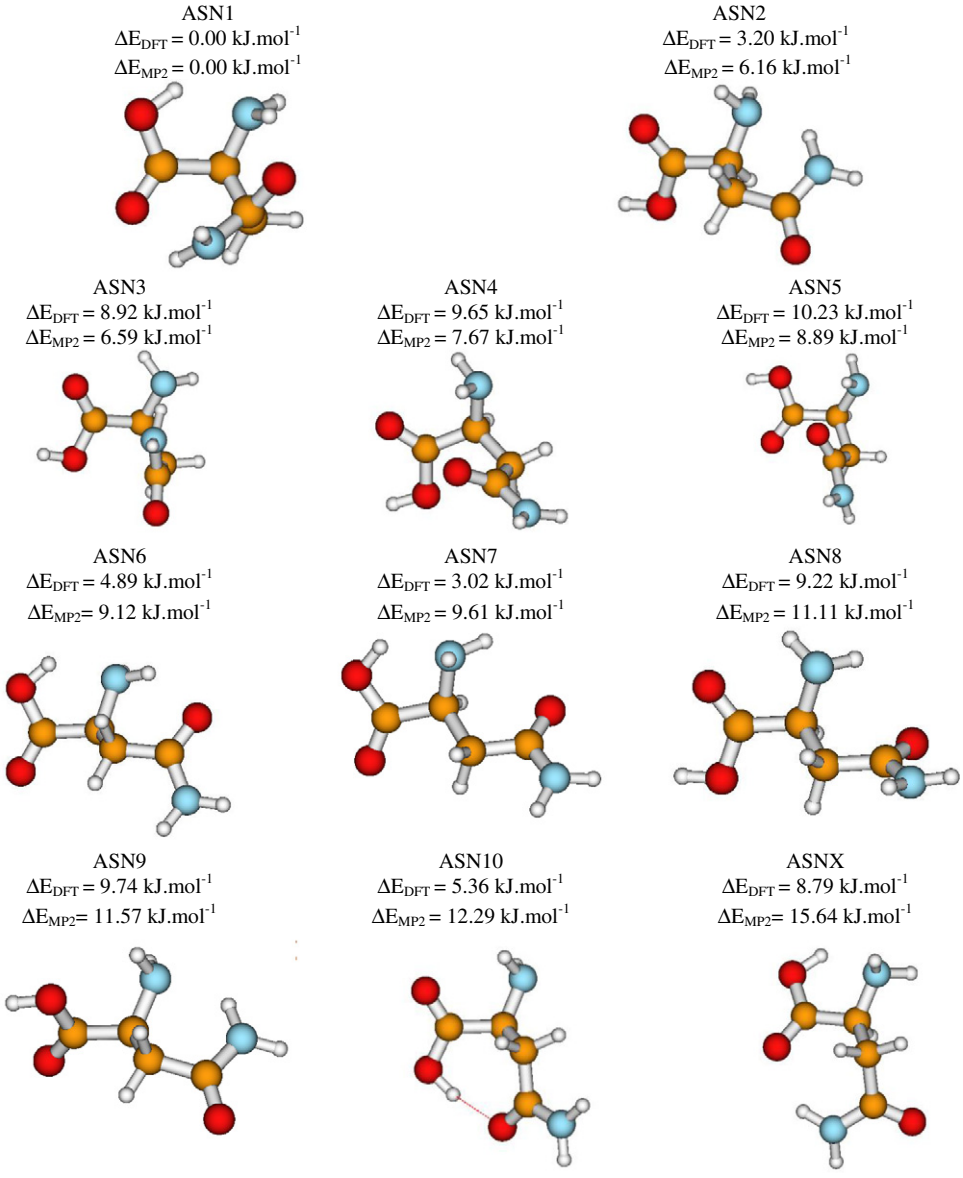

Fig. 2. Optimal geometries and relative energies (DFT(B3LYP)/6-31++G** and MP2/6-31++G**) of the most stable conformations of asparagine.

Table 2
DFT(B3LYP)/6-31++G** and MP2/6-31++G** computed thermodynamical data for asparagine at 298.15 K and 353.00 K: relative zero-point corrected energies (ΔE/kJ.mol^{-1}), formation enthalpies (ΔH°/kJ.mol^{-1}), entropy contributions (TΔS°/kJ.mol^{-1}), Gibbs free energies (ΔG°/kJ.mol^{-1}), rotamerization constants (K_r) and abundances (%) of the 10 most stable MP2 conformations.

Conformation	Type of backbone[a]	ΔE[b]	ΔH°	TΔS°	ΔG°	K_r	%[c]	ΔH°	TΔS°	ΔG°	K_r	%[c]
	DFT											
			298.15 K[d]					353.00 K[e]				
ASN1	I $N^{bb}H...O^{sc}+N^{sc}H...O^{bb}$	0.00	0.00	0.00	0.00	1.00	30.24	0.00	0.00	0.00	1.00	23.03
ASN2	II $N...HN^{sc}$	3.20	4.27	3.46	0.81	0.72	21.79	4.45	4.29	0.16	0.95	21.81
ASN3	II $N...HN^{sc}$	8.92	9.51	1.43	8.08	0.04	1.16	9.68	1.87	7.80	0.07	1.61
ASN4	II	9.65	11.56	4.91	6.66	0.07	2.06	11.95	6.23	5.72	0.14	3.29
ASN5	III	10.23	11.87	5.05	6.82	0.06	1.93	12.22	6.36	5.86	0.14	3.13
ASN6	I $NH...O^{sc}$	4.89	5.47	1.95	3.53	0.24	7.28	5.54	2.37	3.17	0.34	7.83
ASN7	I $NH...O^{sc}$	3.02	4.18	3.62	0.56	0.80	24.16	4.36	4.49	−0.13	1.05	24.07
ASN8	II $NH...O^{sc}$	9.21	11.20	5.36	5.84	0.09	2.87	11.58	6.77	4.82	0.19	4.46
ASN9	III $N...HN^{sc}$	9.74	10.87	4.34	6.54	0.07	2.16	11.08	5.35	5.73	0.14	3.27
ASN10	IV $OH...O^{sc}$	5.36	6.41	2.03	4.38	0.17	5.17	6.56	2.57	3.99	0.26	5.92
ASNX[f]	I $O..HN^{sc}$	8.79	8.91	0.89	8.02	0.04	1.19	8.92	1.06	7.86	0.07	1.58
	MP2											
			298.15 K					353.00 K				
ASN1	I $N^{bb}H...O^{sc}+N^{sc}H...O^{bb}$	0.00	0.00	0.00	0.00	1.00	56.08	0.00	0.00	0.00	1.00	41.43
ASN2	II $N...HN^{sc}$	6.15	7.42	4.23	3.19	0.28	15.50	7.61	5.22	2.39	0.44	18.36
ASN3	II $N...HN^{sc}$	6.58	7.26	1.46	5.80	0.10	5.41	7.43	1.92	5.51	0.15	6.33
ASN4	II	7.67	9.25	3.75	5.50	0.11	6.09	9.61	4.83	4.78	0.20	8.13
ASN5	III	8.89	10.22	3.99	6.23	0.08	4.54	10.53	5.06	5.47	0.15	6.42
ASN6	I $NH...O^{sc}$	9.11	10.37	3.92	6.46	0.07	4.15	10.49	4.78	5.72	0.14	5.89
ASN7	I $NH...O^{sc}$	9.60	10.52	2.87	7.65	0.05	2.56	10.67	3.57	7.10	0.09	3.68
ASN8	II $NH...O^{sc}$	11.11	12.76	4.46	8.30	0.04	1.97	13.10	5.65	7.45	0.08	3.28
ASN9	III $N...HN^{sc}$	11.56	12.92	4.89	8.04	0.04	2.19	13.13	6.02	7.12	0.09	3.67
ASN10	IV $OH...O^{sc}$	12.28	14.33	5.02	9.31	0.02	1.31	14.58	6.22	8.36	0.06	2.40
ASNX[f]	I $O..HN^{sc}$	15.64	16.00	2.16	13.85	0.00	0.21	16.04	2.59	13.45	0.01	0.42

[a] Backbone type I is characterized by an intramolecular $OH...N^{bb}$ H-bond, II by a $N^{bb}H_2...O=C^{bb}$ H-bond, III by a $N^{bb}H_2...O–C^{bb}$ interaction and IV by a $N^{bb}H2...O=C^{bb}$ H-bond.
[b] ZPE corrected energy relative to ASN1: $E_{DFT}=-492.362536$ a.u. and $E_{MP2}=-490.996980$ a.u.
[c] Only taking into account the most stable conformations.
[d] Relative to ASN1. Absolute values for ASN1: $H°_{DFT}=-492.351970$ a.u., $H°_{MP2}=-490.986580$ a.u.; $TS°_{DFT}=0.044916$ a.u., $TS°_{MP2}=0.044496$ a.u.; $G°_{DFT}=-492.396885$ a.u., $G°_{MP2}=-491.031077$ a.u.
[e] Relative to ASN1. Absolute values for ASN1: $H°_{DFT}=-492.348645$ a.u., $H°_{MP2}=-490.983301$ a.u.; $TS°_{DFT}=0.056786$ a.u., $TS°_{MP2}=0.056239$ a.u. ; $G°_{DFT}=-492.405430$ a.u., $G°_{MP2}=-491.039540$ a.u.
[f] ASNX is included in the Table because $\Delta E_{DFT}<10$ kJ.mol−1.

3. Experimental methodology

FT-IR spectra were registered by a Bruker IFS66 spectrophotometer at a resolution of 1 cm^{-1}. Asparagine was sublimated at 353 K out of a small home-made mini-furnace, placed in the cryostat and mixed with a large excess of Ar. During the experiment the temperature of the CsI window was kept at 18 K while the argon pressure in the cryostat was 1.4×10^{-5} mbar. Using these parameters, no decomposition occurred and the yield was sufficiently high to detect asparagine in the matrix. To avoid the presence of water impurities, asparagine was dried in a furnace at 80 °C during 24 h. Asparagine was commercially purchased from FLUKA with a purity over 99.5%. High purity argon gas of Air Liquide (99.99990%) was used for the experiments.

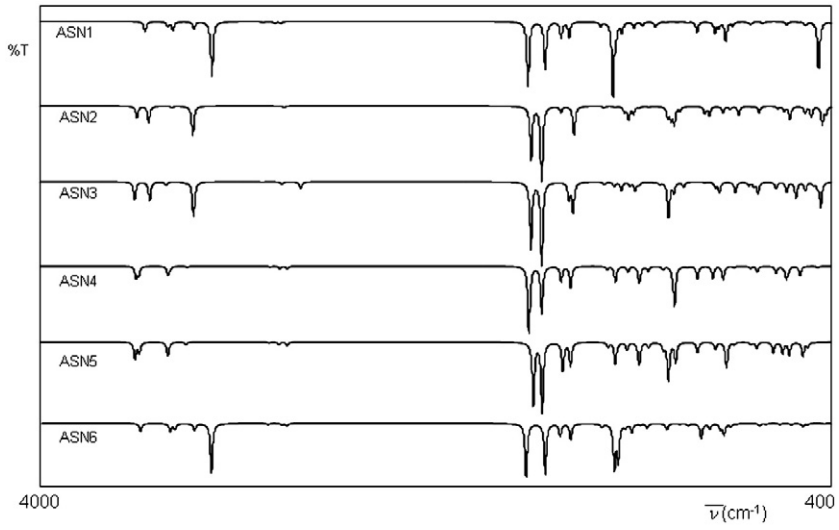

Fig. 3. Theoretical (DFT) IR spectra of the most abundant (MP2) conformations of asparagine.

4. Results

Asparagine has 6 degrees of rotational freedom as shown in Fig. 1. There are three rotational axes in the amino acid backbone, i.e. O=C–OH (a), NC^{α}-C=O (b) and $C^{ca}C^{\alpha}$-NH_2 (c), and three additional ones in the side chain, i.e. $C^{ca}C^{\alpha}$-$C^{\beta}C^{\gamma}$ (d) $C^{\alpha}C^{\beta}$-$C^{\gamma}N$ (e) and $C^{\beta}C^{\gamma}$-NH (f). Variation of all these single-bond rotators results in all the possible conformations. The two values of the dihedral angle (a) results in the syn and anti conformation of the carboxylic acid group. The dihedral angle b can rotate over six values, i.e. 30, 90, 150, 210, 270 and 330°. Threefold rotation is involved for the dihedral angles c, d, e and f. This results in a total set of ($2\times6\times3\times3\times3\times3=$) 972 possible conformations. This large set has first been optimized by Chen et al. [10] at the DFT(B3LYP)/6-311G* level and afterwards at the B3LYP/6-311++G** level of theory. MP2/6-311++G** single point energy calculations were finally performed. The obtained 10 most stable conformations and some additional structures with increased stability due to intramolecular H-bonds were used in the present work as starting structures and these were optimized at the DFT(B3LYP)/6-31++G** level of theory.

The performed optimization resulted in 10 conformations with a DFT energy difference smaller than 10 kJ.mol^{-1} (Table 1). These 10 conformations are mostly similar to those obtained by Chen et al. [10]. Optimization at the MP2/6-31++G** level of theory revealed 7 conformations with an MP2 energy difference smaller than 10 kJ.mol^{-1}. The smaller relative energies and the reversed order for some conformations is due to the fact that in this work MP2 optimizations (Fig. 2) were performed whereas Chen et al. have only performed single point MP2 energy calculations on DFT optimized geometries.

The most stable conformation ASN1 has a OH…N^{bb} H-bond and is stabilized by two additional intramolecular H-bonds N^{sc}H…O=C and N^{bb}H…$O=C^{sc}$. ASN2 has a weak NH_2…O=C H-bond and has extra stability from the N^{sc}H…N^{bb} intramolecular H-bond. These characteristics are also observed for ASN3. ASN4 has the same type of backbone but has no additional H-bond interaction. ASN5 is the most stable conformation with an bifurcated intramolecular NH_2…O–C H-bond. No N^{bb}H..$O=C^{sc}$ intramolecular H-bond is present in ASN4 and ASN5 since the distance between H and O atoms (2.91 and 3.51 Å, respectively) exceeds the sum of de vander Waals radii (2.68 Å) [34]. ASN6 and ASN7 are nearly the same conformations, both with an OH…N^{bb} H-bond in the backbone and an additional NH…$O=C^{sc}$ H-bond. ASN8 has a NH_2…O=C H-bond and a weak additional N^{bb}H…$O=C^{sc}$ H-bond. ASN9 has a NH_2…O(H) H-bond in the backbone and an additional NH…N^{bb} intramolecular H-bond. ASN10 is the most stable conformation with an OH…N^{sc} intramolecular H-bond. Similar to ASN1, ASNX which was not below the 10 kJ.mol^{-1} limit in the study of Chen [10], has the amino acid backbone type I with a typical OH…N^{bb} H-bond and an additional NH…$O=C^{sc}$ H-bond.

The intramolecular OH…N^{bb} H-bond in the most stable conformation is in contrast to previously studied amino acids like glycine [32], alanine [21], cystein [11] or isoleucine [6] in which the most stable conformations contains the bifurcated NH_2…O=C intramolecular H-bond is observed in the most stable form. This can be explained by the presence of the H-bond involved groups in the side chain of asparagine which seemed to have a more stabilizing effect.

The theoretically calculated thermodynamical properties, the rotamerization constants and the relative abundaces of the most stable conformations at room temperature (298 K) as well as at the sublimation temperature used (353 K) are presented in Table 2. The relative order of the Gibbs free energy is, apart from a few exceptions, the same as for the electronic energies. The Gibbs free energy gap between ASN1 and the other conformations is decreased due to the entropy contribution which is the most unfavourable for ASN1. This can be explained by the three intramolecular H-bonds in this conformation, i.e. N^{bb}H…O^{sc}=C, N^{sc}H…O=C^{bb} and O^{bb}H…N^{bb} compared to only one or two intramolecular H-bonds in the other conformations. The MP2 entropy difference between ASN1 and ASN2 is −5.22 kJ.mol^{-1} at the sublimation temperature. This difference is larger than the previously observed entropy differences, i.e. −2.25 kJ.mol^{-1} for isoleucine [6], −4.73 kJ.mol^{-1} for *N*-acetylglycine [4] and −3.91 kJ.mol^{-1} for *N*-acetylalanine [5]. This suggests a stronger intramolecular H-bond between the amino acid backbone and the side chain in asparagine compared to those in the backbone of the other amino acids.

Considering the abundances larger than 5% at the sublimation temperature, which is demonstrated to be reasonable in the past, the DFT abundances predict that four conformations would be present in the argon matrix, i.e. ASN1, ASN2, ASN6 and ASN7. On the other hand, the MP2 abundances predict six abundant conformations, i.e. ASN1-ASN6. The differences in the backbone between these conformations will give rise to spectral differences suitable to identify the conformations in the matrix. Among these six conformations, four groups of conformations will be clearly distinguishable due to the different H-bonds. The theoretical DFT spectra of these six conformations are presented in Fig. 3.

The experimental matrix-isolation FT-IR spectrum of asparagine recorded from 4000 to 500 cm^{-1} is presented in Fig. 4. Although the amino acid was dried to reduce the moisture, it was not totally eliminated, as can be seen in the region 3800–3700 cm^{-1}. Comparison of

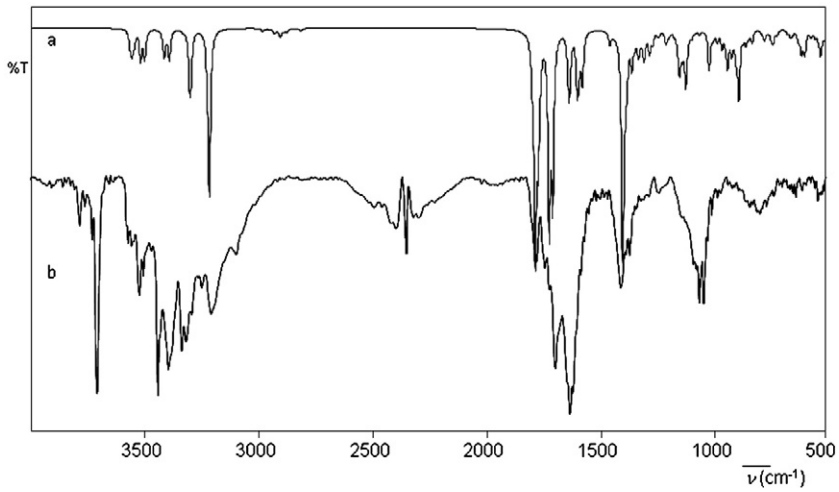

Fig. 4. Theoretical DFT (a) and experimental FT-IR (Ar at 18 K) (b) spectrum of asparagine.

Table 3
Experimentally observed frequencies (cm^{-1}), intensities ($km.mol^{-1}$) and theoretical IR spectral data (DFT(B3LYP)/6-31++G**) for the 6 most abundant conformations of asparagine.

Experimental		Theoretical[a]												
		ASN1		ASN2		ASN3		ASN4		ASN5		ASN6		
$\overline{\nu}$[b]	I[c]	$\overline{\nu}$	I	$\overline{\nu}$	I	$\overline{\nu}$	I	$\overline{\nu}$	I	$\overline{\nu}$	I	$\overline{\nu}$	I	PED[d]
3572	sh					3569	85							ν (OH) (99)
3566	s									3567	70			ν(OH) (99)
								3563	59					ν(OH) (99)
				3559	71									ν(OH) (100)
3550	m							3551	46					$\nu^{as}(NH_2)^{sc}$ (100)
3539	sh											3550	49	$\nu^{as}(NH_2)^{sc}$ (99)
										3548	45			$\nu^{as}(NH_2)^{sc}$ (100)
3516	vs	3522	56											ν^{as} $(NH_2)^{sc}$ (100)
3499	m			3505	100									$\nu^{as}(NH_2)^{sc}$ (100)
						3501	92							$\nu^{as}(NH_2)^{sc}$ (86) + $\nu^{s}(NH_2)^{sc}$ (14)
3435	s					3426	16							$\nu^{as}(NH_2)^{bb}$ (100)
										3421	14			$\nu^{as}(NH_2)^{bb}$ (98)
3425	sh	3418	26											ν^{as} $(NH_2)^{bb}$ (100)
								3418	45					$\nu^{as}(NH_2)^{bb}$ (98)
										3417	48			$\nu^{s}(NH_2)^{sc}$ (99)
												3415	51	$\nu^{s}(NH_2)^{sc}$ (99)
								3408	15					$\nu^{s}(NH_2)^{sc}$ (99)
3400	sh			3399	9									$\nu^{as}(NH_2)^{bb}$ (100)
3390	vs	3395	48											ν^{s} $(NH_2)^{sc}$ (100)
												3394	37	$\nu^{as}(NH_2)^{bb}$ (98)
						3337	4							$\nu^{s}(NH_2)^{bb}$ (100)
										3336	11			$\nu^{s}(NH_2)^{bb}$ (98)
								3330	7					$\nu^{s}(NH_2)^{bb}$ (99)
				3323	1									$\nu^{s}(NH_2)^{bb}$ (98)
3329	m			3305	178									ν^{s} $(NH_2)^{sc}$ (97)
												3304	43	$\nu^{s}(NH_2)^{bb}$ (89)
3311	m					3301	170							$\nu^{s}(NH_2)^{sc}$ (84) + $\nu^{as}(NH_2)^{sc}$ (15)
		3299	39											$\nu^{s}(NH_2)^{bb}$ (99)
												3227	319	ν(OH…) (98)
3201	vs	3218	299											ν(OH…) (98)
1792	sh											1792	342	ν(C=O)^{bb} (82)
1779	sh	1780	353											ν(C=O)^{bb} (82)
1770	s							1776	352					ν(C=O)^{bb} (85)
				1766	323									ν(C=O)^{bb} (86)
						1767	326							ν(C=O)^{bb} (83)
1733	m									1756	262			ν(C=O)^{bb} (86)
1713	m			1718	452									ν(C=O)^{sc} (79)
						1718	407							ν(C=O)^{sc} (78)
								1718	249					ν(C=O)^{sc} (76)
										1716	292			ν(C=O)^{sc} (86)
												1705	327	ν(C=O)^{sc} (73)
1687	vs	1702	260											ν(C=O)^{sc} (72)
1637	sh											1637	81	$\delta(NH_2)^{bb}$ (82)
				1631	35									$\delta(NH_2)^{bb}$ (84)

(continued on next page)

Table 3 (*continued*)

Experimental		Theoretical[a]										
		ASN1		ASN2		ASN3		ASN4		ASN5		ASN6		
1622	vs	1630	88											$\delta(NH_2)^{bb}$ (84)
1610	sh							1629	81					$\delta(NH_2)^{bb}$ (79) + $\gamma(NH_2)^{bb}$ (20)
										1622	118			$\delta(NH_2)^{bb}$ (80) + $\gamma(NH_2)^{bb}$ (20)
1593	sh	1594	83											$\delta(NH_2)^{sc}$ (78)
						1594	80							$\delta(NH_2)^{bb}$ (80) + $\gamma(NH_2)$ (19)
												1589	103	$\delta(NH_2)^{sc}$ (89)
										1587	99			$\delta(NH_2)^{sc}$ (91)
								1586	112					$\delta(NH_2)^{sc}$ (90)
1575	w					1575	145							$\delta(NH_2)^{sc}$ (85)
1559	sh			1571	174									$\delta(NH_2)^{sc}$ (83)
1399	vs	1393	405											δ(OH) (14) + ν(C–O) (12)
												1390	284	δ(OH) (66)
1297	vw			1301	45									δ(OH) (22) + ν(C–O) (14)
						1293	43							δ(OH) (26) + ν(C–O) (17) + δ(CH) (15) + δ(C=O) (11) + $\rho(NH_2)^{bb}$ (11)
1231	w			1231	5									δ(OH) (20) + δ(CH) (12)
										1165	29			$\rho(NH_2)^{bb}$ (28) + γ(CCCC) (25) + $\nu(C^{\alpha}C^{\beta})$ (16) + $\tau(CH_2)$ (15)
		1152	3											$\rho(NH_2)^{bb}$ (29) + $\delta(C^{\beta}C^{\gamma})$ (10)
1130	m									1142	161			δ(OH) (37) + $\delta(C^{\alpha}C^{\beta}C^{\gamma})$ (24) + ν(C–O) (24) + δ(CH) (20)
						1141	172							δ(OH) (39) + ν(C–O) (28)
				1130	75									ν(C–O) (16) + $\rho(NH_2)^{bb}$ (13) + δ(OH) (12)
								1122	28					δ(CCC) (40) + γ(CH) (25) + $\delta(CN^{bb})$ (18) + $\nu(C^{\alpha}C^{ca})$ (14) + $\rho(NH_2)^{bb}$ (11)
						1117	50							$\rho(NH_2)^{sc}$ (47) + $\nu(CN^{sc})$ (16) + $\nu(C{=}O)^{sc}$ (11)
				1115	109									$\rho(NH_2)^{sc}$ (25) + ν (C–O) (18) + δ(OH) (12)
								1114	203					ν(C–O) (36) + δ(OH) (34) δ(CH) (10)
										1109	84			$\delta(C^{ca}C^{\alpha}C^{\beta}C)$ (30) + $\nu(C^{\alpha}C^{ca})$ (21) + $\nu(C^{\alpha}N)$ (21)
1078	w			1089	25									$\nu(NC)^{bb}$ (39)
1067	w					1073	24							$\nu(NC^{\alpha})$ (33) $\delta(C^{ca}C^{\alpha}C^{\beta})$ (17) + γ(CH) (12)
1054	m									1059	1			$\rho(NH_2)^{sc}$ (42) + $\nu(CN^{sc})$ (27)
								1056	5					$\rho(NH_2)^{sc}$ (52) + $\nu(CN^{sc})$ (26) + $\nu(C{=}O)^{sc}$ (11)
												1053	13	$\rho(NH_2)^{sc}$ (36) + $\nu(CN)^{sc}$ (21) + $\nu(NC^{\alpha})$ (11)
999	s											994	98	$\gamma(NH_2)^{bb}$ (28) + τ(CH) (14) + γ(C=O) (12)
974	m					977	3							$\gamma(CH_2)$ (20) + $\nu(C^{\alpha}C^{\beta})$ (18) + γ(CCCC) (13)
				976	44									$\gamma(NH_2)^{bb}$ (14) + $\nu(NC)^{bb}$ (13) + $\nu(C^{\alpha}C^{\beta})$ (10)
961	m			955	57									$\gamma(NH_2)^{bb}$ (24) + $\nu(C^{\alpha}C^{\beta})$ (14)
								940	62					$\gamma(NH_2)^{bb}$ (31) + $\nu(C^{\alpha}C)$ (17) + $\gamma(CH_2)$ (16)
927	w	931	58											$\gamma(NH_2)^{bb}$ (24)
						928	25							$\gamma(NH_2)$bb (16) + $\delta(C^{\alpha}C^{\beta}C^{\gamma})$ (14) + γ(C–O) (13)
909	w	913	30											γ(OH) (23)
						910	52							$\gamma(NH_2)^{bb}$ (30) + $\delta(CH_2)$ (15) + $\tau(CH_2)$ (12) + $\nu(C^{\alpha}C^{\beta})$ (12)
												906	36	$\nu(C^{\beta}C^{\gamma})$ (23) + γ(OH) (18) + $\gamma(C{=}O)^{bb}$ (15)
898	w			894	39									$\nu(C^{\alpha}C^{\beta})$ (18) + $\nu(C^{\beta}C^{\gamma})$ (16)
								893	72					$\gamma(NH_2)^{bb}$ (30) + $\nu(NC^{\alpha})$ (24)
												890	73	γ(OH) (67) + $\gamma(NH_2)^{bb}$ (10)
881	w	881	107											γ(OH) (57)
										878	108			$\gamma(NH_2)^{bb}$ (45) + $\nu(C^{\alpha}N)$ (16) + $\delta(NH_2)^{bb}$ (12)
851	w	849	21											ν $(NC)^{bb}$ (20)
758	m			761	3									$\gamma(NH_2)^{sc}$ (68)
						753	22							$\tau(NH_2)^{sc}$ (52) + $\nu(C^{\beta}C^{\gamma})$ (10)

743	sh					734	56						$\tau(NH_2)^{sc}$ (17) + $\delta(C^{\alpha}C^{\beta}C^{\gamma})$ (13) + δ(C–O) (13) + ν(C–O) (13) + $\nu(NC^{\alpha})$ (11)
726	m			729	39								γ(OH) (23)
654	w					652	33						γ(OH) (27) + $\delta(C^{\alpha}C^{\beta}C^{\gamma})$ (17) + $\gamma(C{=}O)^{bb}$ (10)
641	m							652	37				γ(OH) (24) + δ(C=O) (22) + γ(C=O) (16) + $\delta(C^{\alpha}C^{\beta}C^{\gamma})$ (13)
				644	14								$\delta(C{=}O)^{bb}$ (38) + ν(C–O) (11)
629	m									622	48		$\tau(NH_2)^{sc}$ (21) + $\gamma(C{=}O)^{sc}$ + γ(OH) (19) + $\gamma(CN^{sc})$ (19) + $\tau(CH_2)$ (10)
								621	7				$\tau(NH_2)^{sc}$ (33) + $\gamma(C{=}O)^{sc}$ (25) + $\gamma(CN^{sc})$ (24) + $\tau(CH_2)$ (12)
				615	29								γ(OH) (30) + $\gamma(NH_2)^{sc}$ (39)
								605	66				γ(OH) (45) + $\delta(C{=}O)^{bb}$24)
						604	47						γ(OH) (43) + $\delta(C{=}O)^{bb}$ (23)
601	m	603	18										$\gamma(NH_2)_{sc}$ (54)
										592	53		γ(OH) (40) + δ(C=O) (17)
583	w			589	80								$\delta(C{=}O)^{bb}$ (50)
												583	7 $\tau(NH_2)^{sc}$ (40) + $\delta(C{=}O)^{sc}$ (15)
564	m					562	78						$\delta(C{=}O)^{bb}$ (20) + $\delta(C{=}O)^{sc}$ (14) + γ(OH) (11)
		550	2										$\delta(NCO)^{sc}$ (18) + $\delta(CO)^{bb}$ (13) + δ(C–O) (11)
544	m							543	49				$\delta(C{=}O)^{sc}$ (21) + $\delta(C{=}O)^{bb}$ (17) + γ(OH) (14) + $\delta(CN^{sc})$ (13)
532	m									530	60		δ(C–O) (22) + $\delta(CN^{sc})$ (16)
												530	19 $\delta(C{=}O)^{bb}$ (30) + $\delta(C{=}O)^{sc}$ (29) + $\nu(C^{\beta}C^{\gamma})$ (12)
521	w	520	15										$\delta(CO)^{sc}$ (26) + $\nu(C^{\alpha}C^{\beta})$ (12) + $\delta(CO)^{bb}$ (12)
				520	41								$\delta(C{=}O)^{sc}$ (38)
						519	42						$\delta(CN^{sc})$ (26) + δ(C=O) (19) + $\nu(C^{\beta}C^{\gamma})$ (13)
513	w	514	6										$\delta(C^{\alpha}C^{\beta})$ (24)
												511	7 γ(C=O) (20) + $\tau(NH_2)^{sc}$ (17)
										508	20		δ(C=O) (30) + $\nu(C^{\alpha}C^{ca})$ (20) + $\delta(CN^{bb})$ (18) + $\delta(C^{\alpha}C^{\beta}C^{\gamma})$ (12)

[a] Variable scaling factors for DFT: 0.95 for (X-H); 0.98 for γ and τ; 0.975 for all other modes.
[b] Observed frequency in the matrix-isolation FT-IR spectrum of asparagine.
[c] Relative experimental intensity denoted as vs (very strong), s (strong), m (medium), w (weak), vw (very weak) and sh (shoulder).
[d] Potential energy distribution (%); only contributions >10% are listed.

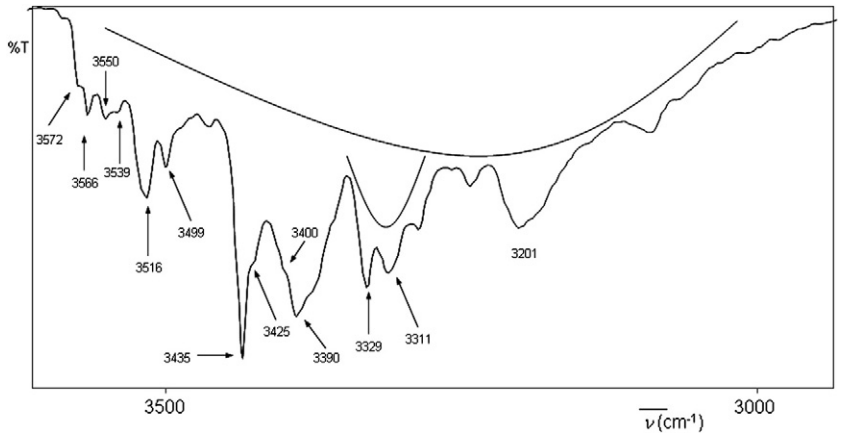

Fig. 5. High frequency region (3600–2900 cm^{-1}) of the FT-IR spectrum of asparagine in Ar at 18 K.

the observed water frequencies with previously reported literature data for water in Ar [3] reveals that the water impurities present are mainly monomeric water, which does not influence the amino acid vibrations. The theoretical spectrum in Fig. 4 is based on the DFT frequencies, taking into account the MP2 abundances of the six most stable conformations. The spectral analysis is performed for three spectral different regions, i.e. 3600–2900 cm^{-1}, 1900–1000 cm^{-1} and 1000–500 cm^{-1}. The most important spectral data are presented in Table 3, a full overview is available in the supporting information.

4.1. 3600–2900 cm^{-1}

The high frequency region of the FT-IR spectrum of asparagine is shown in Fig. 5. In this region the asparagine ν(XH) modes, i.e. one ν(OH) mode, four $\nu(NH_2)$ mode, two $\nu(CH_2)$ modes and one $\nu(C^{\alpha}H)$ mode are situated.

The most important mode located in this region is ν(OH). This mode is involved in an intramolecular H-bond in conformations ASN1 and ASN6. The predicted ν(OH…) frequencies for these conformations are 3218 and 3227 cm^{-1}, respectively, and these are clearly red shifted compared to the non H-bonded ν(OH) modes in ASN2, ASN3, ASN4 and ASN5, predicted at 3559, 3569, 3563 and 3567 cm^{-1}, respectively. The non H-bonded modes are observed in the band at 3566 cm^{-1} with a shoulder at 3572 cm^{-1}. The observed, very broad band ranging from ±3600 to ±2900 cm^{-1} with a maximum around 3200 cm^{-1} can be assigned to the ν(OH…) modes of ASN1 and ASN6. It is not unusual for amino acids with several relatively strong intramolecular H-bonds that such a broad band is observed, which results from several moderately broad ν(OH…) modes of the different H-bonds.

The experimental values of the ν(OH) mode involved or not involved in an OH…N intramolecular H-bond observed for asparagine are comparable by these observed for other amino acids, as indicated in Table 4. This can be a very useful tool to assign these modes in the future for even more complex systems.

Table 4
Experimental values of the ν(OH) and ν(OH…) modes for the most stable conformations and frequency shifts.

Compound	ν(OH) (cm^{-1})	ν(OH…) (cm^{-1})	$\Delta\nu$ (cm^{-1})
Asparagine (this work)	3566	3200	−366
Alanine(21)	3560	3193	−367
Glycine(32)	3560	3200	−360
Isoleucine(6)	3565	3185	−380
Cystein(11)	3570-3540	3330-3270	-±265
Proline(36)	3559	3025	−534

For some of the six conformations, the NH_2 group is involved in an intramolecular H-bond. In that case, $\nu^{as}(NH_2)$ can be better described as the stretching vibration of the free NH group and $\nu^{s}(NH_2)$ as the stretch of the H-bonded group NH…. The reason is that, when a single H-bond H-N-H… is formed, the coupling between the two ν(NH) stretches, which gives rise to the ν^{a} and ν^{as} modes in a free NH_2 group, strongly decreases. The predicted frequencies of $\nu^{as}(NH_2)^{sc}$, i.e. the non H-bonded NH stretch, range from 3551 to 3501 cm^{-1}. The experimental band observed at 3550 cm^{-1} with a shoulder at 3539 cm^{-1} can therefore be assigned to the NH stretch of ASN4, ASN5 and ASN6 with nearly identical theoretical values, i.e. 3551, 3548 and 3550 cm^{-1}, respectively. In view of the large intensity, the $\nu^{as}(NH_2)^{sc}$ mode of the most abundant predicted conformation ASN1 is observed at 3516 cm^{-1} (predicted at 3522 cm^{-1}). The smallest $\nu^{as}(NH_2)^{sc}$ frequencies are predicted for the conformations with intramolecular $N^{sc}H…N^{bb}$ H-bonding, i.e. ASN2 (3505 cm^{-1}) and ASN3 (3501 cm^{-1}). These absorptions are observed probably at 3499 cm^{-1}.

The observed band at 3435 cm^{-1} with a shoulder at 3425 cm^{-1} can probably be assigned to the asymmetric NH_2 stretching modes of the backbone NH_2 group of four of the six conformations present, all predicted between 3426 and 3418 cm^{-1}, and the intensity of this band is easily understood considering the sum of the individual theoretical intensities. The shoulder observed at 3400 cm^{-1} could then be due to the somewhat decreased $\nu^{as}(NH_2)^{bb}$ absorptions of ASN2 and ASN6.

The $\nu^{s}(NH_2)^{sc}$ modes which are not involved in any H-bond are predicted between 3417 and 3395 cm^{-1} and may absorb either at 3425 cm^{-1} or at 3400–3990 cm^{-1}. Only for conformations ASN2 and ASN3 this mode is involved in an $N^{sc}H…N$ intramolecular H-bond which is clearly seen in the values of the theoretical frequencies, i.e. 3305 cm^{-1} (ASN2) and 3301 cm^{-1} (ASN3), both with much larger intensity. These modes are observed in the somewhat broadened band with maxima at 3329 and 3311 cm^{-1}. Due to the H-bond this mode has also a contribution to the broad band ranging from ±3600 to ±2900 cm^{-1}. The $\nu^{s}(NH2)^{bb}$ mode is too weak for conformations ASN2-ASN5 (1–11 km.mol^{-1}). Only for the forms ASN1 and ASN6 an observable intensity is predicted at 3299 and 3304 cm^{-1}, respectively.

The unimportant $\nu(CH_2)$ and ν(CH) absorptions are too weak (predicted intensities smaller than 15 km.mol^{-1}) to be separately observed in the experimental spectrum.

4.2. 1900–1000 cm^{-1}

The spectral region 1900–1000 cm^{-1} (Fig. 6) contains the ν(C=O), the $\delta(NH_2)$ and the δ(OH)as most important modes.

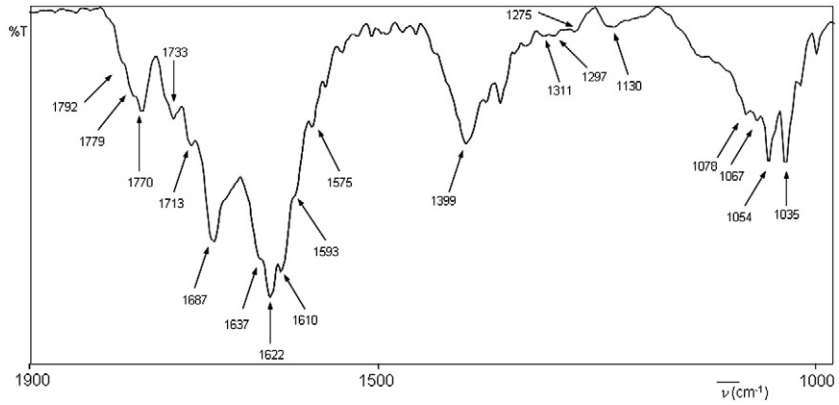

Fig. 6. Frequency region 1900–1000 cm^{-1} of the FT-IR spectrum of asparagine in Ar at 18 K.

The $\nu(C=O)$ modes of the amino acid backbone, denoted as $\nu(C=O)^{bb}$, are observed in the rather complicated band centered at 1770 cm^{-1} with shoulders at 1779 and 1792 cm^{-1}. This assignment is in accordance with the predicted values 1792, 1780, 1776, 1767, 1766 and 1756 cm^{-1} for ASN6, ASN1, ASN4, ASN3, ASN2 and ASN5, respectively. The fact that two shoulders are observed besides the main band suggests that at least three conformations are present in the matrix.

The theoretical frequencies of the amide $\nu(C=O)^{sc}$ mode of the side chain are very similar for conformations ASN2-ASN5, i.e. 1718–1716 cm^{-1}, whereas the frequencies for ASN1 and ASN6 are red shifted to 1702 and 1705 cm^{-1}, respectively, due to the intramolecular H-bond $N^{bb}H\ldots O=C^{sc}$. In the experimental spectrum the former are observed at 1733 and 1713 cm^{-1}, while the bonded $\nu(C=O\ldots)$ mode is observed in the broader, more intense band at 1687 cm^{-1}.

Predicted frequency differences for the $\delta(NH_2)^{bb}$ mode are insignificant (1637–1622 cm^{-1}), except for ASN3 (1594 cm^{-1}) and these modes are observed in the broad band centered at 1622 cm^{-1} with several shoulders, e.g. at 1637 cm^{-1}. The $\delta(NH_2)^{sc}$ modes, predicted between 1594 and 1571 cm^{-1} are observed in the shoulders at 1593 and 1575 cm^{-1}. The assignments of these bands are somewhat tentative because these bands overlap with the δ(OH) mode of the water contamination.

The $\rho(NH_2)^{bb}$ vibration which has potential energy contribution to the modes predicted between 1388 and 1122 cm^{-1} and the $\rho(NH_2)^{sc}$ mode predicted between 1117 and 1053 cm^{-1} are strongly coupled modes. Therefore these modes cannot inform about the H-bonds and are not usable to distinguish between the different conformations.

The δ(OH…) modes involved in an intramolecular $OH\ldots N^{bb}$ H-bond in ASN1 and ASN6 are predicted with large intensity at 1393 and 1390 cm^{-1}. There is a clear red shift and a much larger intensity compared to the other conformations which have significant δ(OH) PED contributions to the modes at 1231 and 1301 cm^{-1} (ASN2), 1141 and 1293 cm^{-1} (ASN3), 1268 and 1114 cm^{-1} (ASN4) and 1279 cm^{-1} (ASN5). In the experimental spectrum, the H-bond involved δ(OH…) mode is observed in the broad band at 1399 cm^{-1} while the weaker bands observed at 1311, 1297 and 1275 cm^{-1} can be assigned to the non H-bonded δ(OH) modes.

4.3. 1000–500 cm^{-1}

The low frequency region of the spectrum of asparagine is shown in Fig. 7. The γ(OH) modes of ASN1 and ASN6, involved in an intramolecular H-bond, are coupled and have major PED contributions to the frequencies predicted at 913 and 881 cm^{-1} (ASN1) and at 890 cm^{-1} (ASN6). These modes are the major origin for the intense, very broad band observed from 950 cm^{-1} to 710 cm^{-1}. The other H-bonded out-of-plane modes $\gamma(NH_2)$ contribute also to the broadening of this band but these are strongly coupled and difficult to analyze. The γ(OH) modes which are not involved in an H-bond are predicted, either at 652 cm^{-1} or between 615 and 592 cm^{-1} and these are tentatively assigned to the bands observed at 629 and 583 cm^{-1}.

This spectral analysis implies that based on the important OH absorptions that (at least) one conformation with and at least 3 conformations without an intramolecular OH…N H-bond are observed in the matrix. The first conformation must be ASN1. The combination with the theoretical details indicates that the other conformations are most likely ASN2, ASN3 and ASN4. There are indications that ASN5 may be present but this conformation has no intense, non-overlapping bands as can be seen in Fig. 3 which makes identification difficult. Since the H-bonding structure in ASN6 is the same as in ASN1, their important vibrations slightly differ. Due to this fact and in combination with the

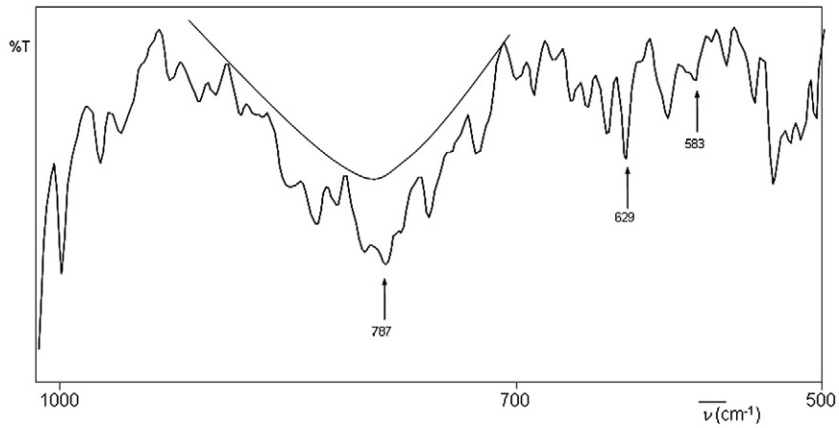

Fig. 7. Low frequency region (1000–500 cm^{-1}) of the FT-IR spectrum of asparagine in Ar at 18 K.

Table 5
Mean IR frequency (cm^{-1}) deviation between experimental and scaled theoretical frequencies.

Amino acid	Mean frequency deviation (cm^{-1})
Asparagine (this work)	7.6
Isoleucine [6]	4.7
Alanine [21]	9.9
Glycine [32]	11.7
Serine [22]	7.6
Alanine [21]	7.6
N-acetyl-glycine [4]	10.2
N-acetyl-alanine [5]	9.5
N-acetyl-proline [7]	12.8
N-acetyl-cysteine [8]	5.5

overwhelming abundance of ASN1, is it reasonable to assign these bands to ASN1.

The obtained mean frequency deviation, $\overline{\Delta\nu} = \overline{|\nu^{exp} - \nu^{the}|}$, is 7.6 cm^{-1} indicating a good agreement between the experimental and the theoretical DFT frequencies. This value is comparable with earlier obtained deviations of less complex amino acids and derivates, as indicated in Table 5.

5. Conclusions

The conformational landscape of asparagine was investigated by optimizations at the B3LYP/6-31++G** level of theory and this resulted in 10 conformations with $\Delta E_{DFT} < 10$ kJ.mol^{-1}. Compared to a previous theoretical study one new conformation was discovered. Further optimization at the MP2/6-31++G** level resulted in 7 conformations with $\Delta E_{MP} < 10$ kJ.mol^{-1}. The most stable conformation contains three intramolecular H-bonds, i.e. C=O^{sc}…HN^{bb}, C=O^{bb}…HN^{sc} and OH^{bb}…N^{bb}. Due to these three H-bonds, this conformation is the most stable form at both levels of theoretical approach.

The order of the Gibbs free energies is, apart from a few exceptions, comparable with the order of the electronic energies. The energy gap between ASN1 and the other conformations is decreased because ASN1 is the only stable conformation with three intramolecular H-bonds with an unfavourable entropy contribution TΔS°. Comparison of this entropy term to other amino acids with only a H-bond interaction in the backbone suggests a stronger H-bond interaction between the side chain and the backbone in asparagine.

At the sublimation temperature of 353 K, the DFT method predicts four and the MP2 method six conformations to be present in the experimental matrix-isolation spectrum. Among these six, three have a different kind of amino acid backbone and additional H-bonds, i.e. 1) an OH…N^{bb} H-bond in the backbone combined with one NH…O^{sc} or two additional C=O^{sc}…HN^{bb}, C=O^{bb}…HN^{sc} H-bond in the side chain; 2) a bifurcated NH_2…O=C H-bond in the backbone combined with no or one additional N…HN^{sc} in the side chain and 3) a conformation containing only a NH_2…O–C H-bond in the backbone.

This makes it possible to identify the particular types of backbone and the particular types of additional H-bond for the most intense predicted modes. The identification of these H-bond involved modes demonstrates the presence of at least four (ASN1-ASN4) conformations in the matrix and suggests the presence of ASN5, although it is very difficult to assign each observed band to a particular mode of a particular conformation. Therefore we were not able to estimate the experimental abundances of each particular conformation as was earlier performed for isoleucine [6], *N*-acetylglycine [4], *N*-acetylalanine [5] of *N*-acetylcystein [8], also because the H-bond involved modes are broadened with the consequence that the most interesting bands could not unambiguously be integrated. For the most abundant conformation ASN1 the mean frequency deviation of 7.6 cm^{-1} demonstrates that the matrix-isolation FT-IR technique, supported by theoretical calculations can be used to investigate very complicated vibrational spectra of amino acids.

Supplementary data related to this article can be found online at doi:10.1016/j.bpc.2012.03.006.

Acknowledgements

This research was funded by the Department of Chemistry of the University of Leuven and was conducted utilizing the high performance computational resources provided by the University of Leuven, http://ludit.kuleuven.be/hpc.

References

[1] C. Aleman, J. Puiggali, Conformational preferences of the asparagine residue. Gas-phase, aqueous solution, and chloroform solution calculations on the model dipeptide, The Journal of Physical Chemistry. B 101 (1997) 3441–3446.
[2] A.D. Becke, Density-functional exchange-energy approximation with correct asymptotic-behavior, Physical Review A 38 (1988) 3098–3100.
[3] R.M. Bentwood, A.J. Barnes, W.J. Orville-Thomas, Studies of intermolecular interactions by matrix-isolation vibrational spectroscopy – self-association of water, Journal of Molecular Spectroscopy 84 (1980) 391–404.
[4] B. Boeckx, G. Maes, Comparison of the conformational behavior of amino acids and N-acetylated amino acids: a theoretical and matrix-isolation FT-IR study of N-acetylglycine, Journal of Physical Chemistry A 116 (2012) 1956–1965.
[5] B. Boeckx, G. Maes, Estimation of the rotamerization constants of different conformations of N-acetylalanine: a theoretical and matrix-isolation FT-IR study, Spectrochimica Acta Part A 86 (2012) 366–374.
[6] B. Boeckx, W. Nelissen, G. Maes, A potential energy surface and matrix-isolation FT-IR study of isoleucine, J. Phys. Chem A, 116 (2012) 3247–3258.
[7] B. Boeckx, R. Ramaekers, G. Maes, The influence of the peptride bond on the conformation of amino acids: a theoretical and FT-IR matrix-isolation study on *N*-acetylproline, Journal of Biophysical Chemistry 159 (2011) 247–256.
[8] B. Boeckx, R. Ramaekers, G. Maes, A theoretical and matrix-isolation FT-IR investigation of the conformational landscape of N-acetylcysteine, Journal of Molecular Spectroscopy 261 (2010) 73–81.
[9] J. Casado, F.J. Ramirez, J.T.L. Navarrete, Vibrational-spectra and assignments of amino-acid L-asparagine, Journal of Molecular Structure 349 (1995) 57–60.
[10] M.L. Chen, Z.J. Huang, Z.J. Lin, Ab initio studies of gasphase asparagine conformers, Journal of Molecular Structure (THEOCHEM) 719 (2005) 153–158.
[11] J.C. Dobrowolski, M.H. Jamroz, R. Kolos, J.E. Rode, J. Sadlej, Theoretical prediction and the first IR matrix observation of several L-cysteine molecule conformers, ChemPhysChem 8 (2007) 1085–1094.
[12] N.V. Dokholyan, J.M. Borreguero, S.V. Buldyrev, F. Ding, H.E. Stanley, E.I. Shakhnovich, Identifying Importance of Amino Acids for Protein Folding from Crystal Structures, in: W.C. Charles (Ed.), Methods in Enzymology Macromolecular Crystallography, Part D, Academic Press, 2003, pp. 616–638.
[13] M.J. Frisch, G.W. Trucks, H.B. Schlegel, G.E. Scuseria, M.A. Robb, J.R. Cheeseman, J.A. Montgomery, T. Vreven, K.N. Kudin, J.C. Burant, J.M. Millam, S.S. Iyengar, J. Tomasi, V. Barone, B. Mennucci, M. Cossi, G. Scalmani, N. Rega, G.A. Petersson, H. Nakatsuji, M. Hada, M. Ehara, K. Toyota, R. Fukuda, J. Hasegawa, M. Ishida, T. Nakajima, Y. Honda, O. Kitao, H. Nakai, M. Klene, X. Li, J.E. Knox, H.P. Hratchian, J.B. Cross, V. Bakken, C. Adamo, J. Jaramillo, R. Gomperts, R.E. Stratmann, O. Yazyev, A.J. Austin, R. Cammi, C. Pomelli, J.W. Ochterski, P.Y. Ayala, K. Morokuma, G.A. Voth, P. Salvador, J.J. Dannenberg, V.G. Zakrzewski, S. Dapprich, A.D. Daniels, M.C. Strain, O. Farkas, D.K. Malick, A.D. Rabuck, K. Raghavachari, J.B. Foresman, J.V. Ortiz, Q. Cui, A.G. Baboul, S. Clifford, J. Cioslowski, B.B. Stefanov, G. Liu, A. Liashenko, P. Piskorz, I. Komaromi, R.L. Martin, D.J. Fox, T. Keith, M.A. Al-Laham, C.Y. Peng, A. Nanayakkara, M. Challacombe, P.M.W. Gill, B. Johnson, W. Chen, M.W. Wong, C. Gonzalez, J.A. Pople, Gaussian 03, Revision B.05, 2003.
[14] H.L. Gordon, H.C. Jarrell, A.G. Szabo, K.J. Willis, R.L. Somorjai, Journal of Physical Chemistry 96 (1992) 1915–1921.
[15] A.L. Heaton, P.B. Armentrout, Experimental and theoretical studies of potassium cation interactions with the acidic amino acids and their amide derivatives, The Journal of Physical Chemistry. B 112 (2008) 12056–12065.
[16] A.L. Heaton, V.N. Bowman, J. Oomens, J.D. Steill, P.B. Armentrout, Infrared multiple photon dissociation spectroscopy of cationized asparagine: effects of metal cation size on gas-phase conformation, Journal of Physical Chemistry A 113 (2009) 5519–5530.
[17] Z.J. Huang, Z.J. Lin, Journal of Physical Chemistry A 109 (2005) 2656–2659.
[18] B. Imperiali, K.L. Shannon, K.W. Rickert, Role of peptide conformation in asparagine-linked glycosylation, Journal of the American Chemical Society 114 (1992) 7942–7944.
[19] A. Kaczor, I.D. Reva, L.M. Proniewicz, R. Fausto, Importance of entropy in the conformational equilibrium of phenylalanine: a matrix-isolation infrared spectroscopy and density functional theory study, Journal of Physical Chemistry A 110 (2006) 2360–2370.
[20] T. Kimura, N. Matubayasi, H. Sato, F. Hirata, M. Nakahara, Enthalpy and entropy decomposition of free-energy changes for side-chain conformations of aspartic acid and asparagine in acidic, neutral, and basic aqueous solutions, The Journal of Physical Chemistry. B 106 (2002) 12336–12343.

[21] B. Lambie, R. Ramaekers, G. Maes, On the contribution of intramolecular H-bonding entropy to the conformational stability of alanine conformations, Spectrochimica Acta Part A 59 (2003) 1387–1397.
[22] B. Lambie, R. Ramaekers, G. Maes, Conformational behavior of serine: an experimental matrix-isolation FT-IR and theoretical DFT(B3LYP)/6-31++G** study, Journal of Physical Chemistry A 108 (2004) 10426–10433.
[23] C.T. Lee, W.T. Yang, R.G. Parr, Development of the Colle–Salvetti correlation-energy formula into a functional of the electron-density, Physical Review B 37 (1988) 785–789.
[24] B. Li, R.T. Borchardt, E.M. Topp, D. VanderVelde, R.L. Schowen, Racemization of an asparagine residue during peptide deamidation, Journal of the American Chemical Society 125 (2003) 11486–11487.
[25] P. Lund, Nitrogen Metabolism in Mammalian, Applied Science, Barking, 1981.
[26] N.M. Luscombe, R.A. Laskowski, J.M. Thornton, Amino acid–base interactions: a three-dimensional analysis of protein–DNA interactions at an atomic level, Nucleic Acids Research 29 (2001) 2860–2874.
[27] C. Moller, M.S. Plesset, Note on an approximation treatment for many-electron systems, Physical Review 46 (1934) 618–622.
[28] M. Muzomwe, B. Boeckx, G. Maes, O.E. Kasende, Discrimination between O–H…N and O–H…O=C complexes of 3-methyl-4-pyrimidone and methanol. A matrix-isolation FT-IR and theoretical DFT/B3LYP investigation, South African Journal of Chemistry 64 (2011) 23–33.
[29] S.E. O'Connor, B. Imperiali, Conformational switching by asparagine-linked glycosylation, Journal of the American Chemical Society 119 (1997) 2295–2296.
[30] R.J. Petrella, M. Karplus, Proteins-Structure Function and Bioinformatics 54 (2004) 716–724.
[31] J.L. Radkiewicz, H. Zipse, S. Clarke, K.N. Houk, Accelerated racemization of aspartic acid and asparagine residues via succinimide intermediates: an ab initio theoretical exploration of mechanism, Journal of the American Chemical Society 118 (1996) 9148–9155.
[32] R. Ramaekers, J. Pajak, G. Maes, On the intramolecular H-bond entropy contribution to the stability of glycine conformations, Asian Chemistry Letters 2 & 3 (2004) 203–209.
[33] H. Rostkowska, L. Lapinski, M.J. Nowak, Analysis of the normal modes of molecules with D-3h symmetry infrared spectra of monomeric s-triazine and cyanuric acid, Vibrational Spectroscopy 49 (2009) 43–51.
[34] R.S. Rowland, R. Taylor, Intermolecular nonbonded contact distances in organic crystal structures: comparison with distances expected from van der Waals radii, Journal of Physical Chemistry 100 (1996) 7384–7391.
[35] L.E. Snyder, J.M. Hollis, R.D. Suenram, F.J. Lovas, L.W. Brown, D. Buhl, An extensive galactic search for conformer-II glycine, The Astrophysical Journal 268 (1983) 123–128.
[36] S.G. Stepanian, I.D. Reva, E.D. Radchenko, L. Adamowicz, Conformers of nonionized proline. Matrix-isolation infrared and post-Hartree-Fock ab initio study, The Journal of Physical Chemistry A 105 (2001) 10664–10672.
[37] S.G. Stepanian, I.D. Reva, E.D. Radchenko, M.T.S. Rosado, M.L.T.S. Duarte, R. Fausto, L. Adamowicz, Matrix-isolation infrared and theoretical studies of the glycine conformers, Journal of Physical Chemistry A 102 (1998) 1041–1054.
[38] M.K. Van Bael, J. Smets, K. Schoone, L. Houben, W. McCarthy, L. Adamowicz, M.J. Nowak, G. Maes, Matrix-isolation FTIR studies and theoretical calculations of hydrogen-bonded complexes of imidazole. A comparison between experimental results and different calculation methods, Journal of Physical Chemistry A 101 (1997) 2397–2413.
[39] L.N. Vauquelin, P.J. Robiquet, La découverte d'un nouveau principe végétal dans le suc des asperges, Annales de Chimie 57 (1806) 88–93.
[40] X. Zhou, H. Chung, M.A.A., M. Rhiel, D.W. Murhammer, Selective measurement of glutamine and asparagine in aqueous media by near-infrared spectroscopy, American Chemical Society (1996) 116–132.